2011-04-28

Investigating the properties of the ZIP4 M3M4 domain in the presence and absence of zinc

Tuong-Vi T. Nguyen
Worcester Polytechnic Institute

Investigating the properties of the ZIP4 M3M4 domain in the presence and absence of Zn^{2+}

By

Tuong-Vi Nguyen

A Thesis

Submitted to the Faculty of the

WORCESTER POLYTECHNIC INSTITUTE

In partial fulfillment of the requirements for the

Degree of Master of Science

In Biochemistry

April 2011

APPROVED:

Dr. Robert Dempski, Major Advisor

Dr. Kristin Wobbe, Head of Department

Abstract

Zinc is the second most abundant transition metal in biological systems. This cation is required for the catalytic activity of hundreds of enzymes which mediate protein synthesis, DNA replication and cell division. Despite the central importance of zinc in cellular homeostasis, the mechanism of zinc uptake, compartmentalization and efflux is unknown. Recently, a family of proteins, called ZIP, has been shown to control zinc uptake. Mutations in one of the genes coding for these proteins (ZIP4) can lead to potentially life-threatening diseases like *Acrodermatitis Enteropathica* and high levels of ZIP4 have been detected in patients suffering from pancreatic cancer. Therefore our goal is to investigate the mechanism of ZIP4 transport and regulation.

It was previously shown that the intracellular loop between transmembrane III and IV (M3M4) of ZIP4 is ubiquitinated in the presence of high intracellular zinc which lead to protein degradation. Our initial hypothesis was that the large intracellular domain of ZIP4 (M3M4) is a sensor which detects the intracellular concentration of zinc and regulates the surface expression of ZIP4. In order to test this hypothesis we expressed and purified the M3M4 domain to examine the ability of M3M4 to bind zinc. Our results have demonstrated that M3M4 binds zinc with a 2:1 zinc:protein stoichiometry with nanomolar affinity. We have also shown that upon binding of zinc, M3M4 undergoes a large conformational change.

Acknowledgements

First and foremost, I would like to extend my warmest gratitude to Dr. Robert Dempski, my advisor, mentor and friend. I am extremely grateful to be a member of his lab. The knowledge obtained during the last two years from his laboratory far exceeds that which is written in this thesis.

I would like to thank Dr. Kristin Wobbe for her support and open door policy whenever we need help.

I would like to Professor Jose Arguello and his lab members for their help and support.

I would like to thank my lab mates (Ryan, Sagar, Olga, and Fei) for enriching my experience here at WPI.

I would like to thank The Arvid Anderson Fellowship for funding my research.

I would like to thank Dr. Patrick Arsenault for helping me settle into the lab during my first year here.

Lastly, I would like to thank my family and friends for their constant support and positive encouragement.

Table of Contents

Table of Figures

1. Introduction

Zinc is the second most abundant transition metal found in biological systems[1]. Zinc plays a crucial role in many biological pathways. It is involved in growth and development, immune function, lipid metabolism, and neurological development[1,2,3,4]. ZIP proteins are a family of zinc transporters that are responsible for the influx of zinc uptake and cytosolic zinc release. Dependent on the functional role of ZIP transporters, some ZIP proteins are ubiquitously expressed and others are tissues-specific. ZIP transporters play a crucial role in maintaining zinc homeostasis. For example, mutations in the ZIP4 transporter result in the genetic disorder *acrodermatitis enteropathica* (AE). This disease is characterized by the cell's inability to uptake zinc[5,6]. AE can lead to death if left untreated, though a zinc supplement can reverse this disorder[5,6]. ZIP4 also play a role in pancreatic cancer as it was recently shown that ZIP4 was overexpressed in patients with pancreatic cancer[7]. In mice, mZIP4 is essential for embryonic development stages. Mutations in the mZIP4 gene can lead to a more severe consequence. Complete loss of mZIP4 functions in mice could lead to embryonic lethality[5].

Although many zinc transporters that influx and efflux zinc have been identified, the exact mechanism of zinc is transport is still unclear. Therefore, the study of how zinc is transported in and out of the cells is of great importance. The overall goal of this project is to investigate the mechanism in which ZIP4 is regulated. The intracellular loop between transmembrane 3 and transmembrane 4 (M3M4) has been shown to be the site for ubiquitination in response to elevated intracellular zinc level[8]. In addition, there is a lysine residue (K463) that is highly conserved among ZIP family protein. Lysine has been known as the site for ubiquination[9]. Our initial hypothesis is that the M3M4 domain binds zinc which induces a conformational change to expose the lysine residue for ubiquitination. In order to test this hypothesis we expressed and purified the M3M4 domain and examined the ability of M3M4 to bind zinc.

1.1 The importance of zinc

Zinc is an essential element that is involved in many biochemical processes. Zinc is most concentrated in the prostate and part of the eyes but is also found in the brain, muscle, bones, kidney, and liver[1]. Zinc is required for the catalytic activity of more than 300 enzymes. For example, the zinc finger, found in hundreds of proteins, is a sequence specific motif that chelates at least one zinc ion and has been found in proteins involved in many aspects of gene regulation in eukaryotes[10]. Zinc also plays an important role in protein synthesis, immune function, wound healing, DNA synthesis, RNA transcription, and cell division[2]. Over one billion people in developing countries are suffering from zinc deficiency. The symptoms for zinc deficiency include severe anemia, growth retardation, hypogonadism, skin abnormalities, geophadia and mental lethargy[11]. The first reported study of the importance of zinc in humans was in 1961 when Prasad describe symptoms of men in Iran suffering from zinc deficiency [11].

The most common factor that leads to zinc deficiency is dietary uptake but hereditary defects can also lead to zinc deficiency. *Acrodermatitis enteropathica* (AE) is the most well-known hereditary disease caused by zinc deficiency in humans. AE can lead to death if left untreated[12]. AE is caused by mutations in a gene that encodes for the ZIP4 protein[13,14,15]. ZIP4 influxes zinc into the cells in enterocytes and pancreatic cells which are the main site for zinc absorption[16,5,17]. Mutations in ZIP4 lead to the malfunction of the protein. This results in a reduced level of total zinc concentration in cells [7, 13, 14].

Zinc also has an adverse effect in many aspects of innate and adaptive immunity. Zinc deficiency can lead to thymic atrophy, alteration in thymic hormones, lymphopenia, and compromising of cellular and antibody-mediated responses[1, 3, 4]. In adaptive immunity, zinc deficiency can cause the decline of T-cell function. Zinc is required as a cofactor for proper function of thymulin, a hormone that is essential for the proliferation and proper function of T-cells, and in zinc deficient mice, the number of active thymulin is decreased which decreases the number of circulating T-cells[1]. In innate immunity, zinc deficiency reduces natural killer (NK) cell lytic activity whereas zinc supplementation improves NK cells function[1].

In the brain, zinc is found at many glutamatergic nerve terminals and is crucial for brain function. It was recently shown that presynaptic release of zinc causes amyloid formation in Alzheimer disease (AD) mouse model[18]. Studies have shown that AD mouse with ZnT3 (a zinc exporter) knockout enhances the formation of soluble amyloid-β[18].

1.2 Zinc regulations

Zinc can be toxic if the concentration is too high. Numerous studies have shown that one of the key factors that induced neuronal cell deaths is the rise of cellular free zinc that is release from permeation of synaptic zinc or release of zinc from intracellular vesicles in neurons[17]. Therefore proper regulation machinery for zinc is required to keep zinc at physiological level. The primary site for the mechanisms of zinc homeostasis is in the gastrointestinal tracts[19, 20]. This is where zinc is absorbed and excreted. Tissue and cellular redistribution also play a role in maintaining zinc at physiological level [20]. Zinc homeostasis is coordinated through regulation of specific proteins involved in the uptake, efflux, and intracellular compartmentalization. The exact mechanisms of how zinc is regulated and coordinated are unknown. However, zinc homeostasis appears to be coordinated through metallothioneins, transmembrane transporters, and cation diffusion facilitators (Figure 1)[19, 21, 22].

Metallothioneins (MTs) are intracellular, low molecular metal-binding proteins that are rich in cysteine[21]. They have a high affinity for metals; predominantly zinc, copper, or cadmium[21]. Mammalian MTs are single-chain polypeptides that have highly conserved cysteine residues and each MT molecule can incorporate up to 7 divalent cations and 12 monovalent copper atoms[19, 21]. Expression of MTs is ubiquitous but most MTs are concentrated in the liver, kidney, and pancreas. The primary role of MTs has not yet been identified but studies have shown that they might play a role in regulation of absorbance and secretion of zinc in the intestines[19]. In zinc-depleted animals, MTs enhances its zinc binding capability indicating a possible role in keeping a basal level of intracellular zinc when zinc is

depleted [21, 23]. MTs act both as a zinc reservoir protein in zinc-replete conditions and zinc buffering protein in zinc-deplete conditions[24].

The cellular zinc concentration is also regulated by transporter. There are two major families of zinc transporter, the ZnT and ZIP family. The ZnT [solute-linked carrier 39 (SLC30)] family is known to efflux zinc across the membrane into vesicles or out of the cells[16, 19, 23]. The ZIP (Zrt- and Irt-like proteins) family is known to mediate zinc influx across the membrane into the cytoplasm [23, 25]. Both members of these families are expressed ubiquitously. More will be discussed on zinc transporters in the following sections. Recently, there is some evidence to support the existence of a Na^+/Zn^{2+} exchanger in neurons. The Na^+/Zn^{2+} exchanger works with a stoichiometry of 3 Na^+ to 1 Zn^{2+}. This promotes a Zn^{2+} efflux against a 500-fold cellular gradient[17].

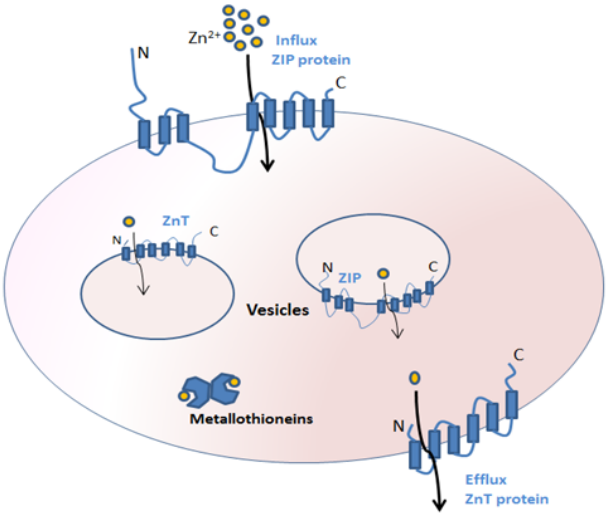

Figure 1: Schematic of zinc intracellular homeostasis.
Zinc is regulated by transporters that are involve in the influxing and effluxing of Zn^{2+}.

1.3 Zinc transporters

Zinc transporters are required for zinc transport. The first identified mammalian zinc transporter was ZnT1 in 1995 by Findley and Palmiter[26]. The human transporters are designated as SLC30A (ZnT) and SLC39A for (ZIP) and the rodent transporters are designated as slc30a and slc39a respectively. A total of twenty-five zinc transporters have been discovered within the last decade, nine of which belong to the ZnT family and the other fourteen belong to the ZIP family[17, 19, 26]. Table 1 gives a summary of the properties of most of ZnT and ZIP transporters.

ZnT family sequences are homologous among human. They vary in sizes; most ZnT transporters have six transmembrane domains with the N-terminus and C-terminus in the cytoplasm[16,19].

Transmembrane domain I, II, and V are amphiphatic and are highly conserved among the family. In between transmembrane IV and V, there is a histidine-rich loop that is also conserved among ZnT[16, 23]. ZnT transporters are widespread to different regions of the body and each play a crucial role in zinc transport. For example, ZnT-1 has been shown to reduce the toxicity of Zn^{+2} in rat neurons[18]. ZnT-1 expression is dependent on the Zn^{+2} concentrations through the transcription factor MTF-1[17, 27]. The mechanism of how ZnT-1 is able to maintain a low Zn^{+2} concentration in the cells is unknown.

The ZIP family is further divided into four subfamilies according to sequence homology. Most ZIP transporters have eight transmembrane domains with both N-terminal and C-terminal in the extracellular side or extravesicular[16]. The most conserved region in the ZIP family is between transmembrane domain IV and V[16]. ZIP transporters increase cytoplasmic [Zn^{+2}] by promoting extracellular zinc uptake and vesicular zinc release. The expression of ZIP transporters are tissue specific. However, the mechanism in which ZIP protein transports zinc across the membrane is still unclear. It has recently been shown that ZIP expression and activity is dependent on zinc availability[8, 28, 29]. ZIP4 transporter whose mutations caused *acrodermatitis enteropathica* belongs to the LZT subfamily of ZIP family[30].

Table 1: Properties of Zinc Transporters

	Expression Pattern	Distribution	Functions and Regulations	References
ZnT-1 SLC30A1	Ubiquitous	Cellular plasma membrane	Cellular zinc exporter, overexpression increases efflux of Zn and lower the zinc intracellular steady state. Regulated by dietary zinc and tissue specificity	[16,26]
ZnT-2 SLC30A2	Small intestine, kidney, placenta, pancreas, testis, vesicles, and mammary gland	Vesicles, lysosomes	Overexpression reduces zinc and reduces cell toxicity at high level of zinc. May function as zinc storage or down regulation absorption.	[31,16, 17]
ZnT-3 SLC30A3	Hippocampus, cerebral cortex, ependyma of mouse spinal cord	Synaptic vesicle membranes	Knockout results in synaptic Zn^{+2} deficiencies.	[16, 17, 32]
ZnT-4 SLC30A4	Mammary gland, brain, kidney, human PMC42 cells,	Intracellular vesicles, and trans golgi	934 C->T mutation results in lethal milk syndrome in mice. Exact functions is still unknown	[16, 17, 33]
ZnT-5 SLC30A5	Endocrine pancreas, ovary, prostate, and testis	Apical membrane Complex with ZnT-5	Mediate zinc uptake Response to zinc could be mediated by MTF1	[16, 17, 34]
ZnT-6 SLC30A6	Liver, brain, and small intestine	Not uniform Complex with ZnT-6	May involve in pathogenesis of Alzheimer's Disease	[17, 25, 35]
ZnT-7 SLC30A7	Small intestine, liver, retina, spleen, kidney, and lung	Golgi	Import zinc into vesicles Might be regulated by zinc level	[16, 17, 36]
ZnT-8 SLC30A8	Pancreas β-cell	Insulin secretory vesicles	Overexpression increase glucose-induced insulin secretion	[17, 37, 38]
ZIP1 SLC39A1	Small intestine, pancreas, prostate, visceral yolk, THP1 cells	Plasma membrane, intracellular vesicles	Participate in zinc uptake Use zinc complexes as substrates	[16, 39,25, 24 23, 38 17, 22 19, 24]
ZIP2 SLC39A2	liver, spleen, small intestine	Plasma membrane	Involve in zinc homeostasis, facilitate zinc uptake Regulates by HCO_3^-	[16, 40]
ZIP3 SLC39A3	Bone marrow, mammary gland, pancreas, prostate, and spleen	Intracellular vesicles	Mediate zinc reuptake and cellular retention in mammary gland,	[16, 41,25 24, 40 23 19, 26]
ZIP4 SLC39A4	Jujenum and duodenum	Apical membrane	Mediate zinc influx Regulates by zinc concentration Mutations caused acromatitis enteropathica	[5, 16, 42]
ZIP5 SLC39A5	Intestine, pancreas, visceral yolk sac	Basalateral membranes when zinc is not limited	During zinc deficiency, ZIP5 remove zinc from the blood Response to zinc availability	[16, 42, 43]
ZIP6 SLC39A6	Breast, prostate, placenta, kidney, pituitary gland, and corpus callosum	Plasma membrane lamellipodiae	Expression is stimulated by estrogen Associate with breast cancer	[16, 44]
ZIP7 SLC39A7	Ubiquitous	ER, Golgi	Transport zinc into the cytosol Response to zinc availability	[45]

1.4 ZIP4 Transporters

ZIP4 plays in an important role in maintaining physiological zinc level by influxing zinc into cells in the intestine. The ZIP4 (SLC39A4) gene has been mapped to chromosome region 8q24.3[15]. The gene (GenBank RefSeq: AK025537) covers about 4.5 kb and is comprised of 12 exons and 11 introns. There are two different ZIP4 isoforms; they differ only in their amino and carboxyl termini. The most abundant isoform (NM_30849) is 2,192 base pairs long and encodes a 68 kb 647-amino acids protein[46]. The other isoform is the result of alternative splicing which encodes a 626-amino acid protein[46]. The main difference between isoform 1 and isoform 2 is that isoform 1 contains a signal peptide at the N-terminal. The ZIP4 gene belongs to a subfamily of ZIP family called LZT family (LIV-1 subfamily of ZIP zinc transporter) which is made up of most of the mammalian ZIP protein (ZIP4-8, ZIP10, ZIP 12-14), all of which transport zinc ions[19, 47]. ZIP4 is highly expressed in the kidney, small intestines, stomach, colon, jejunum, and duodenum which are the main sites for zinc uptake and reabsorption[15, 42, 46]. ZIP4 consists of eight transmembrane domains with both N-terminal and C-terminal domain in the extracellular side of the cell (figure 2). The extracellular N-terminal domain of ZIP4 makes up about 50% of the entire sequence. Regions in transmembrane IV and V are the most conserved among transporters in the same family[13]. Transmembrane V contains the highly conserved motif HEXPHEXGD which is similar to the catalytic zinc-binding site of metalloproteases suggesting that ZIP4 might have another function[45, 47]. ZIP4 intercellular loop between transmembrane domain III and IV has a histidine-rich motif (^{436}-CGHSSHSHGGHSH-^{448}) that is very similar to the zinc binding site in metalloproteases and other zinc binding proteins[2, 8].

AE is a rare autosomal recessive disorder that was recently been mapped to chromosomal region 8q24.3 which encodes for the ZIP4 transporter [13, 15]. AE is a result of zinc malabsorption and severe zinc deficiency [15]. Mutations in ZIP4 prevent zinc from being influxed into enterocytes, which is the main site for zinc absorption. AE is characterized by skin lesions, alopecia, failure to thrive, and

diarrhea[15, 46]. The symptoms can appear as early as weaning and symptoms can persist and spontaneous remission might occur at young age. AE can be fatal if left untreated; fortunately, AE symptoms can be reverse by supplementary zinc[13, 15].

ZIP4 have recently been shown to play an important role in pancreatic cancer. Studies have shown that ZIP4 is over expressed in pancreatic cancer cells[7]. The overexpression of ZIP4 increases the proliferation of pancreatic cancer cells and promotes pancreatic tumor growth in mice[7]. The knock-down of ZIP4 gene by RNAi decreased the level of pancreatic cancer growth and enhanced the survival rate of mice with pancreatic cancer xenografts[48].

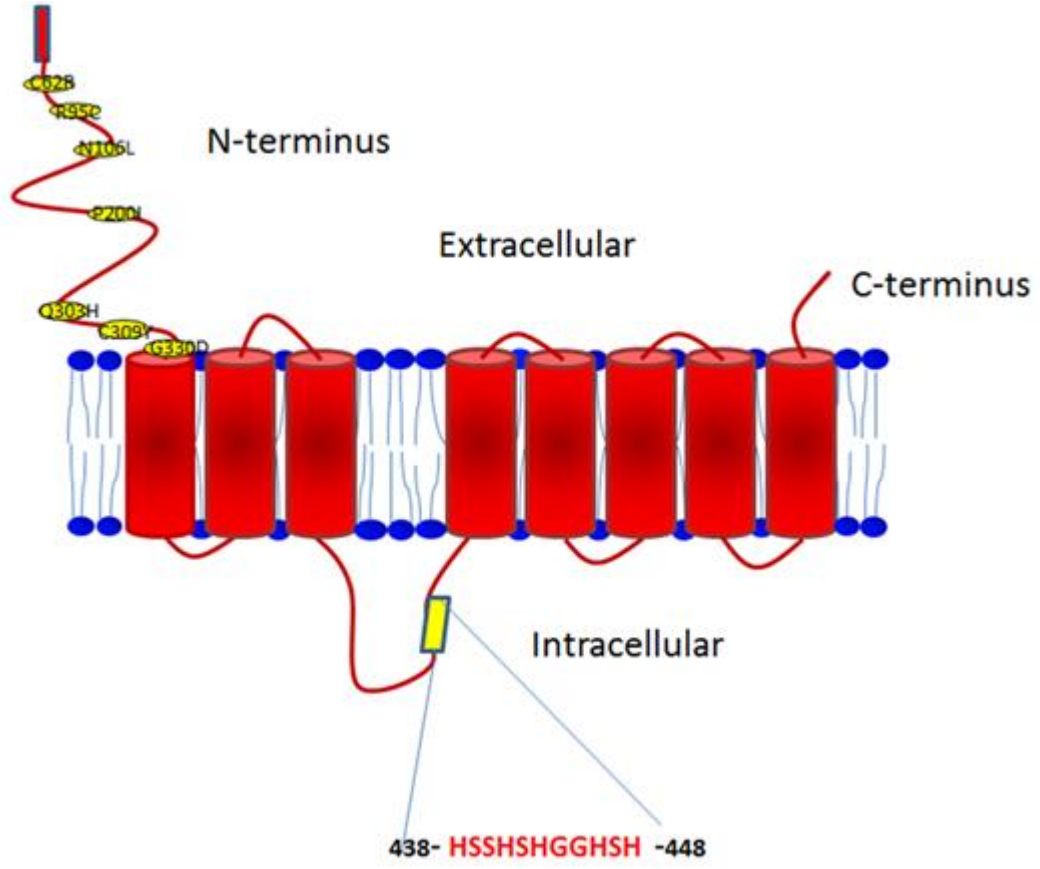

Figure 2: ZIP4 transporters
ZIP4 transporter consists of 8 transmembrane domains and an extracellular N-terminus domain that make up 50% of the entire transporter. Both the N-terminus and C-terminus are extracellular. ZIP4 have a long loop between transmembrane domain III and IV, this loop contains a histidine-rich motif that is found in other transporters. Some mutations on the extracellular N-terminus affecting ZIP4 functions are shown.

Andrews and co-workers[49] mutated the Zip4 gene in mice and showed that homozygous offspring embryos die in 10 days. The heterozygous offspring at 10 days of pregnancy shows a range of abnormalities. When compared to the wild-type embryos, the heterozygous offspring vary in size and morphology, some were smaller and some showed severe growth retardation. Some of the embryos even show irregular craniofacial development. These post-implantation death and embryo damages suggest that Zip4 expression is restricted to the visceral endoderm cells and visceral yolk sac. Unfortunately, the damages that are caused by Zip4 mutation cannot be reversed by supplementing excess zinc to the mother [5, 49].

The mechanism in which ZIP4 is regulated is still unclear. Studies in mice showed that ZIP4 transcription level was not regulated by zinc [42] but the expression level of ZIP4 was zinc-dependent. Recently, some data have emerged to show how ZIP4 is regulated. ZIP4 surface expression is zinc dependent. When the cell is lacking zinc, ZIP4 accumulates at the apical membrane waiting to uptake zinc into the cells. When there is a high level of zinc, ZIP4 undergoes endocytosis and is circulating in the cytoplasm until it is needed[28].

Another mechanism involves the large extracellular N-terminal domain. The N-terminals domain of ZIP4 makes up half the size of the transporter. The N-terminal domain contains a high number of cysteines and histidines which suggest that zinc binds here. During prolonged zinc deficiency, a 37 kDa protein was detected using western blot as the majority form of ZIP4 instead of a full length 68 kDa protein. Data have shown that during prolonged zinc deficiency, the extracellular N-terminal domain was truncated and accumulated as a peripheral membrane protein; the other half is recycled back to the apical membrane[6]. After truncation, the N-terminus domain is loosely associated with the peripheral membrane whereas the processed ZIP4 peptide remained as an integral membrane protein. The processed ZIP4 protein still retained its zinc uptake function when zinc is at normal level. The cleavage is

site specific. AE mutation site G340D in ZIP4 significantly diminished the processing of this ZIP4 protein followed by C319Y and Q313H mutations[6].

When there is a very high level of zinc (10-20 μM) ZIP4 is subjected to degradation. The histidine-rich motif in the loop between transmembrane III and IV (M3M4) plays a crucial role in the degradation of ZIP4. In a zinc-depleted environment, ZIP4 is ubiquitinated at the M3M4 region and subsequently degraded by the lysosomal and proteosomal pathway. It was suggested that a highly conserved lysine (K463) is the site for ubiquitination and the histidine-rich motif (^{438}-HSSHSHGGHSH-^{448}) is required for this process to occur[8, 28]. We hypothesize that this M3M4 domain, in the presence of excess zinc, binds zinc and induced a conformational change which expose the conserved lysine for ubiquitination.

2. Materials and Methods

2.1 Plasmid construction

Our initial aim was to express three domains of ZIP4. The first domain is the extracellular N-terminal with signal sequence (WS) starting at nucleotide 101 to 1081 (protein residues 1 to 327).The second region is the extracellular N-terminal domain without signal sequence (NS) starting at nucleotide 178 to 1081 (protein residues 23 to 327).The third region is the cytoplasmic topological domain between transmembrane three and transmembrane four (M3M4), nucleotides 1360 to 1594 (protein residues 423 to 499). The SLC39A4 gene plasmid was obtained from Invitrogen and the primers were designed according to the SLC39A4 sequence in GenBank (Accession # AK025537). The first plasmid used for protein expression in *E. coli* was pTYB2 (NEB) that has a chitin binding domain tag at the C-terminus. The plasmid was under the control of a T7 promoter and has a built-in ampicillin resistance gene. Primers were design for this plasmid with a *NheI* cut site at the 5'-end and *EcoRI* cut site at the 3'- end (Table 2). The second plasmid was pPR-IBA1 (IBA) with a strep-tag II (WSHPQFEK) at the C-terminus. PPR-IBA1 (IBA) is a strong bacteriophage T7 promoter-based expression vector that contains the ampicillin resistance gene. Primers were designed to carry two unique cut sites 5'-KpnI and 3'-NcoI.

Table 2: PCR Primers

ZnForWS pTYB2	5'- AGTCCTGCTAGC CTG GTC TCG CTG GAG CTG GGG- 3'
ZnForNS pTYB2	5' - AGTCCTGCTAGC CCG CCT GCT GGT CTG CTG AGC -3'
ZnRev pTYB2	5' GTCACGGAATTCCATGTGACTGGCTGAGCTGGTCCTG -3
M3M4For pTYB2	5' – AGCATGGACCGCGGCTGCCCAGGGACCCGGAGGAC-3'
M3M4Rev pTYB2	5'- AGATAAGGCCATGGATAGGGCAGTAGCCTCAACTCAG -3'
M3M4 Forward pPR-IBA1	5'AGCATGGAGGTACCCTGCCCAGGG ACCCGGAGGAC-3'
M3M4 reverse pPR-IBA1	5'-AGATAAGG CCATGGCCATAGGGCAGTAGCCTCAACTCAG-3'
NS Forward pPR-IBA1	5' - ACGGTCGGA GGTACC TCCCCGCCTGCTGGTCTGCTG -3'
NS Reverse pPR-IBA1	5' -ACGGTCGGA CCATGGATACCTCTCTGACTGGCTGAGC -3'
WS Forward pPR-IBA1	5'- ACGGTCGGAGGTACCGCGTCCCTGGTCTCGCTGGAGC-3'
WS Reverse pPR-IBA1	5' -ACGGTCGGA CCATGGATACCTCTCTGACTGGCTGAGC -3'

The genes for M3M4, NS, and WS were amplified by PCR with the primers in Table 2. PCR was performed using *Pfu* DNA polymerase (Stratagene) and the conditions were as follows:

Segment	Number of cycles	Temperature	Duration
1	1	94-98°C	1 minute
2	25-30	94-98°C (T_m-5 °C) = 50 °C 72 °C	30 seconds 30 seconds 2 minutes
3	1	72 °C	10 minutes

The PCR products were purified using Macherey-Nagel NucleoSpin Extract II kit and verified by 1% agarose gel electrophoresis.

The restriction enzymes *NheI* (NEB) and *EcoRI* (NEB) were used to digest the 5' and 3' ends of the PCR product and the pTYB2 vector. *KpnI* (NEB) was used to digest the 5' end and *NcoI* (NEB) was used to digest the 3' ends of the PCR product and pPR-IBA1 vector. The digestion reactions were incubated for two hours in a 37°C water bath. After digestion and purification, the digested PCR products were inserted into the plasmids with DNA according to table 1.

Table 1: Ligation reaction

5x ligation buffer	2 µl
Vector (100 ng/µl)	1 µl
DNA inserts (100 ng/µl)	3 µl
T4 DNA ligase (Invitrogen)	1 µl
ddH_2O	3 µl
Total volume	10 µl

The ligation samples were incubated at room temperature for 5 minutes and placed on ice to stop the reaction. The ligated reactions were transformed into 50 µl of XL-10 Ultra competent cells (Agilent Technology); all transformation procedures were performed according to manufacturer's recommendation. The transformed cells were plated on LB plates (1% (w/v) tryptone, 0.5% (w/v) yeast extract, 1% sodium chloride, and 1.5% (w/v) agar) with 100 ng/µl ampicillin and incubated at 37°C

overnight. Single colonies from plates were picked from the plates and inoculated in 5 ml LB media (1% (w/v) tryptone, 0.5% (w/v) yeast extract, and 1% (w/v) sodium chloride and 100 ng/ µl ampicillin) cultures. The cultures grew overnight (12-16 hours) on a shaker at 37°C. The cultures were harvested and the plasmids were purified using the Machery-Nagel Nucleospin Plasmid miniprep kit. The purified plasmids were sent out to MGH DNA Sequencing Core for sequencing. Successfully ligated plasmids were designated as pTNS, pTWS, and pTM3 for genes inserted into pTYB2 plasmids and pRNS, pRWS, and pRM3 for genes inserted into pPR-IBA1 plasmid.

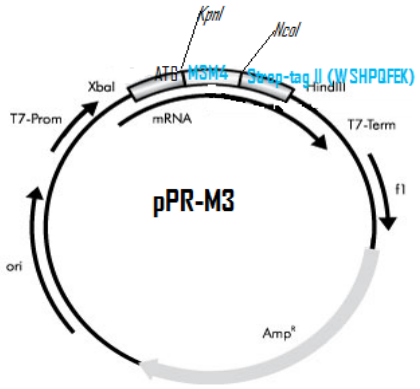

Figure 3: Schematic of pPR-M3 vector*. M3M4 gene is inserted in the MCS of pPR-IBA1 (IBA) with Strep-tag fused at the C-terminus of the gene.*

2.2 Expression of proteins with chitin binding protein

All three ligated vectors in pTYB2 (pTNS, PTWS, and pTM3) were transformed into the *E. coli* strain BL21 (star) DE3 pLysS 1240 (Invitrogen) for expression. Colonies were picked to inoculate a 5 ml start-up LB media culture containing 100 ng/µl ampicillin, 50 ng/µl spectinomycin, and 34 ng/µl chloramphenicol and grew overnight at 37°C. The start-up cultures (1 mL) were used to inoculate a 50 mL LB media culture containing all three antibiotics. The cultures were allowed to grow to OD 0.6-0.8. The cultures were induced with 0.1 mM, 0.2 mM, 1 mM or 2 mM IPTG for 4 hours, 8 hours, or overnight.

The cells were harvested by centrifugation at 5000 g at 4°C for 15 minutes. The supernatants were discarded and the pellets were resuspended in 2 mL of lysis buffer (50 mM Tris-Cl, pH 8.0, 1 mM EDTA, 100 mM NaCl, 1 mM Pefabloc SC) and ultra-sonication (Fisher Scientific Sonic Dismembrator Model 100) was applied at power level 3.5 for 3 burst of 30 seconds with 30 seconds of rest on ice in

between each burst. Samples were kept on ice at all times during sonication. The samples were spun down at 15000 g at 4°C for 15 minutes. Protein samples were loaded on SDS-PAGE.

2.3 Detection of chitin binding protein by western blotting

The proteins were run on SDS-PAGE and transferred to a nitrocellulose membrane via the wet method transfer. Briefly, the transfer was run at 100 V for 1 hour in transfer buffer (see below) with 20% methanol. The membrane was blotted overnight with Tris buffer saline (TBS) with 1% blotto. The membrane was washed 3 x 10 minutes with TBS-0.5% Tween 20. The membrane was incubated with chitin binding protein polyclonal primary antibody (IBA) (1:5000 dilutions) for 1 hour. The membrane was washed with TBS-Tween-20 for 3 x 5 minutes and incubated with 10 µl of phosphatase secondary antibody. The membrane was developed with 10 ml of phosphatase substrate (NBT/BCIP solutions) (KPL).

2.4 Expression of proteins with strep-tag

The pPR-M3 plasmid and pPR-NS were transformed into the *E. coli* strain BL21 (star) DE3 pLysS 1240 (Invitrogen) for protein expression. The cells were grown in 1 liter of autoinduction media [50] on a shaker at 37°C overnight. The media contains 100 ng/µl ampicillin, 50 ng/µl spectinomycin, and 34 ng/µl chloramphenicol. The cells were harvested by centrifugation at 5000 *g* at 4°C for 15 minutes. The pellets were resuspended in buffer W (10 mM Tris-Cl, pH 8.0, 150 mM NaCl, and 1 mM EDTA). The cells were lysed by ultra-sonication on ice at power level 7.5 for 7x 30 seconds with 30 seconds of rest on ice in between each burst. Cell debris and proteins were separated by centrifuging at 15000 *g* at 4°C for 15 minutes. The supernatant was saved and cell debris was discarded. Protein samples were run on SDS-PAGE.

2.5 SDS-Polyacrylamide gel electrophoresis

Protein samples (20 µl) were combined with 4 µl of 6x sample buffer (100 mM Tris, pH 6.8, 2% SDS, 5% ß- mercaptoethanol, 15% glycerol, and 0.012% (w/v) bromophenol blue) and incubated at 90°C for 5 minutes to denature the proteins. The samples were loaded on the wells of a 12% SDS-polyacrylamide gel. The gel was run at 35 mA until the loading dye reached the bottom of the gel (approximately 2-3 hours).

To stain the gel, the stacking gel was removed and discarded; the separate gel was transferred into a gel box and 50 ml of Coomassie staining solution (0.025% Coomassie blue G-250, 10% acetic acid, 90% ddH_2O). The gel was stained at room temperature on a shaker for 1 hour. The staining solution was poured off and 50 ml of destaining solution (7% glacial acetic acid, 5% methanol in ddH_2O) was added. The gel was left to destain until bands were visible.

2.6 Checking for insoluble protein aggregations

Proteins were expressed in small (50 mL) cultures (see section 2.4 for details) and the cells were harvested by centrifugation at 1000 g for 15 minutes at 4°C. The supernatant were discarded and the pellets were weighed. The cells were resuspended in approximately 3 mL of lysis buffer (50 mM Tris-Cl, pH 8.0, 1 mM EDTA, 100 mM NaCl, 1 mM Pefabloc SC) to every wet gram of cells. Lysozyme (300 µg/mL) was added the suspension and stirred for 30 minutes at 4°C. After 30 minutes of incubation, 1% (v/v) Triton X-100 was added and ultrasound sonication was applied for three burst of 30 seconds at power level 3 with 30 seconds of rest on ice in between each burst. The suspensions were placed at room temperature. DNAse I (10 µl) and 10 mM $MgCl_2$ were added and the suspensions were stirred at room temperature for 15 minutes. The suspensions were centrifuged at 15000 g for 15 minutes; the supernatant were separated from the pellets. The pellets were resuspended in equal volume of lysis buffer as the supernatant. Aliquots of 10 µl of the supernatant and resuspended pellet were loaded on SDS-PAGE and further analyzed by western blotting.

2.7 Optimizing protein expression for protein NS

Several different conditions were used to optimize the expression level of NS protein due to its high level of expression in the aggregate form. Freshly transformed BL 21 colonies were used to inoculate a small 5 ml starter culture, grown overnight at 37°C. The starter culture (1 ml) was used to inoculate a 50 ml culture and allowed it to grow to OD of 0.6 to 0.8. All cultures were grown in LB media. The conditions to grow and induce these cultures were as followed:

Cultures	Growth Temp (°C)	Induction Temp (°C)	[IPTP] (mM)	Induction Time (hrs)	[$ZnCl_2$]
Control	37	37	---	Overnight	---
B	37	37	0.1	Overnight	---
C	37	37	1	Overnight	---
D	37	37	2	Overnight	---
E	37	28	1	Overnight	---
F	28	28	1	Overnight	---
G	28	37	1	Overnight	---

The Strep-tag manufacturer (IBA) also recommended growing the starter culture at lower temperature which can also help protein to solubilize. Here, fresh transformed BL 21 colonies were used to inoculate 5 mL starter cultures and grew in a shaker at 25°C overnight. The starter cultures (1 ml) were used to start up a 50 ml culture. The conditions for the cultures were as followed:

Cultures	Growth Temp (°C)	Induction Temp (°C)	[IPTP] (mM)	Induction Time (hrs)	[$ZnCl_2$] (µM)
Control	37	37	---	Overnight	---
A2	37	37	1	4	---
A3	37	25	1	7	---
A4	37	37	1	4	50
A5	37	25	1	7	50

The cells were harvested and lyses according to the protocol for inclusion bodies in section 2.6. NS proteins, both soluble and nonsoluble fractions, were analyzed by western blotting.

2.8 Analysis of the expressed strep-tag fused proteins by western blot

The proteins on the SDS-PAGE were transferred to a PVDF membrane using the wet method in 25 mM Tris, 20 mM Glycine, and 20% (v/v) methanol for 1 hour at 100V, constant voltage. The membrane was blotted with 20 ml of 3% (v/v) BSA, 0.5% Tween-20 in PBS buffer (4 mM KH_2PO_4, 16 mMNa_2HPO_4, 16 mM NaCl) overnight at 4°C. The membrane was washed with 3 x 5 minutes with 40 ml of PBS-Tween (PBS buffer with 0.1% Tween-20). After the last wash, the membrane was incubated in 10 ml of PBS-Tween with 10 µl of biotin blocking buffer (IBA) for 10 minutes to block off the biotin carboxyl carrier protein of *E. coli*. The membrane was washed twice with PBS Tween for 1 minute each. The membrane was incubated for 1 hour in 10 ml of PBS Tween with a 1:8000 dilution of Strep-tactin conjugated alkaline phosphatase antibody (IBA). The membrane was washed 3 x 1 minute with PBS Tween-20 and 2 x 1 minute with PBS. The membrane was developed by BCIP/NBT Phosphatase substrate (1-component) solutions (KPL) until bands were visible. The membrane was washed with water and let sit at room temperature to dry.

2.9 Affinity Purification for M3M4 protein

Fresh colonies were picked and inoculated in 5 mL LB media cultures to grow overnight at 37°C in a shaker incubator. The overnight cultures were used to inoculate 2 liters of autoinduction media. The antibiotics used were 100 ng/µl ampicillin, 34 ng/µl chloramphenicol, and 50 ng/µl spectinomycin. The culture was grown overnight at 37°C in a shaker. The cells were harvested by centrifugation at 5000 g for 15 minutes at 4°C. The supernatant was discarded and the cell pellet was resuspended in 20 mL of washing buffer (100 mM Tris-Cl pH 8.0, 150 mM NaCl, and 1 mM EDTA). The cells were burst by ultra-sonication with 10 burst of 30 seconds on ice at power level 7.5 with 30 seconds rest on ice in between. The cell debris was separated from the supernatant by centrifugation at 15000 g for 15 minutes at 4°C. The cell debris was discarded and supernatant were used to run on the affinity column.

The affinity column was packed with 2 ml of Strep-Tactin resin (IBA) to purify 50 ml of reaction mixtures. The column was equilibrated with 25 ml washing buffer (100 mM Tris-Cl pH 8.0, 150 mM NaCl, and 1mM EDTA). The resin in the column was then removed and incubated with the proteins in a 50 ml conical tube for 2 hours at 4°C on a shaker. The column was repacked with the bound protein-resin and was washed with 25 ml of washing buffer. The target proteins were eluted in 1 ml fractions with 15 ml of elution buffer (100 mM Tris-Cl pH 8.0, 150 mM NaCl, 1 mM EDTA, and 2.5 mM desthiobiotin) and 10 µl of the sample fractions were loaded on SDS-PAGE to check for purity.

The concentration of protein was checked via Bradford's assay [51]. The protein was then further purified through a chelex-100 column to remove any trace of divalent cation metals in the solution. The proteins were concentrated using Amicon Ultra-4 centricon (Millipore), centrifuged at 4000 rpm in a tabletop centrifuge, and the same method was used to switch buffer. In this case, the protein we were trying to purify has a molecular weight of 11 kDa so the selected centricon pour size was 3000 NMWL. In order to properly switch buffer and remove any trace of EDTA from solution, the protein must be washed at least 3 times with the replacing buffer.

2.10 N-terminal sequencing

Protein samples were sent to Iowa State Protein Facility for N-terminal sequencing. M3M4 protein (2 µM) was run on SDS-PAGE and transferred to PVDF membrane. The gel was allowed to polymerize overnight prior to usage. The membrane was stained with Coomassie blue staining solution for one hour. The membrane was destained using 25% acetic acid/ 50%methanol/ ddH_2O. The bands corresponding to M3M4 were excised and placed in an Eppendorf tube.

2.11 Atomic Absorbance Spectroscopy

The samples contained 1 µM M3M4 protein and 5 µM zinc (II) chloride in tris buffer (20 mM Tris-Cl, 150 mM NaCl pH 7.4). The final sample volume was 5 mL. Samples for AAS were prepared by incubating M3M4 protein with 5x excess zinc (II) chloride for 15 minutes at room temperature. The excess zinc was removed by washing the samples three times with 10 times excess protein buffer (20 mM Tris, 150 mM NaCl pH 7.4) using a centricon (Millipore). The other method used for removing excess zinc was to pass the samples through a Sephadex G-25 column, 250 µl protein samples for every 1 ml of Sephadex resins. The Sephadex beads were equilibrated in water for at least one night prior to usage. Nitric acid (metal trace) (1 mL) was added to the samples and incubated at 70°C for one hour and let sit overnight at room temperature. Prior to running the sample, 250 µl of hydrogen peroxide was added and the volume was raised to 5 ml with Tris buffer. Perkin Elmer Flame Atomic Absorbance Spectrophotometry was used for zinc scanning. A zinc standard curve ranging from 0 – 1000 ppb was constructed using the commercially available zinc standard solution (Fluka Analytical, 1000 mg/L).

2.12 Native gel electrophoresis

The conformational changes of M3M4 protein in the presence and absence of zinc (II) was examined by native gel electrophoresis. M3M4 protein (2 µM) was incubated with 5x excess zinc (II) chloride for 15 minutes at room temperature. Loading buffer was added to the protein sample and 10 µl of the sample was loaded on a 10% polyacrylamide gel (no SDS). A pure M3M4 protein with the same concentration (here instead of zinc (II) chloride solution, tris buffer was added) was loaded on the gel. A non-denaturing marker (Sigma #MWND500) which was composed of five different proteins (α-Lactalbumin from bovine milk, Carbonic Anhydrase from bovine erythrocytes, Albumin from chicken egg white, Albumin from bovine serum, and Urease from Jack bean) was also loaded on a separate lane. The gel was run at 25 mA, constant amperes, until the loading dye reached the bottom of the gel. The gel

was stained by Coomassie blue G-250 solutions (0.025% (w/v) Coomassie blue G-250 in 10% acetic acid, ddH_2O).

2.13 Interaction of Zinc Binding by Fluorescence Spectroscopy

The interaction of zinc binding was examined by fluorescence spectroscopy using either the Perkin Elmer LS-55 spectrofluorometer or Perkin Elmer VICTOR 1420 multilabel counter. For the LS-55, the experiment was carried out by stepwise addition of zinc (II) chloride to 2 µM of protein, after the addition of zinc; the sample was left to incubate for 5 minutes before each measurement. The emission spectra were recorded with excitation at 280 nm and emission range from 300 to 800 nm with 1 nm steps at 25°C.

In addition, the fluorophore Fluozin-1 was used to detect free zinc (II). Perkin Elmer VICTOR 1420 multilabel counter was used for this experiment. First, a standard curve was established for the fluorescence of Fluozin-1 with increasing concentration of zinc (II). This was done on a 96-well plate, zinc (II) concentrations range from 0-300 µM were added to 1 µM of Fluozin-1, and buffer (20 mM Tris-Cl, pH 7.4, 150 mM NaCl) was used to bring up solution to 100 µl total. Conditions for the spectrofluorometer were as followed:

Protocol name	Fluozin
Label technology	Prompt fluorometry
CW-lamp filter name	F485
CW-lamp filter slot	A5
Second meas. CW-lamp filter name	F485
Second meas. CW-lamp filter slot	A5
Emission filter name	F535
Emission filter slot	A5
Second meas. emission filter name	F535
Second meas. emission filter slot	A5
Measurement time	0.1 second
Emission aperture	Normal
CW-lamp energy	15000
Second measurement CW-lamp energy	30961

For protein binding reading, 1 µM M3M4 protein was added to 1 µM Fluozin-1 and zinc (II) was added with concentrations ranged from 0 – 3 µM. Protein buffer (20 mM Tris-Cl, pH 7.4, 150 mM NaCl) was used to bring solution up to 100 µl.

The K_d of Fluozin-1 to zinc was determined by best fitting the standard curve with the simple ligand binding one site saturation program in SigmaPlot using the following equation:

$$f = \frac{B_{max} * [Zn]_{free}}{K_d + [Zn]_{free}}$$

Where f is defined as fluorescence intensity of Fluozin-1 binding to zinc ions, B_{max} is the number of binding site (B_{max}=1), and $[Zn]_{free}$ is the concentration of free zinc. The K_d was determined to be 11.98 µM and this was the value used for calculations of $[Zn^{2+}]_{free}$ and [Protein-Zn^{2+}] complex.

2.14 Secondary structure circular dichroism (CD)

All samples were prepared in trizma buffer (10 mM Trizma pH 7.8, 30 mM NaCl). All samples and buffer were passed through a Chelex-100 column. Phosphate buffer is the best buffer to use for CD but as phosphate precipitates with Zn^{2+} we could not use it. The CD analysis was carried out with M3M4 protein concentration ranges from 5 µM to 50 µM. For zinc binding analysis, 5x excess zinc were added to 30 µM protein and incubated for 15 minutes prior to scanning. All the scans were run on Jasco J715 spectropolarimeter equipped with a Peltier thermostated sample holder for thermal melts. All scans were done in triplicates. The data were analyzed by using K2d analysis algorithm (http://geneura.ugr.es/k2d/k2d.html). The CD scanning parameters were as followed:

Sensitivity standard	100 mdeg
Start	270 nm
End	190 nm
Data pitch	0.5 nm
Scanning mode	Continuous
Scanning speed	20 nm/min
Response	8 seconds

Band width	2.0 nm
Accumulation	3
Temperature	4°C
Cell 1 mm for	200 µl

Melting curves for M3M4 protein bound to zinc and unbound to zinc were also performed. The M3M4 protein concentration was 10 µM in trizma buffer (20 mM Trizma, pH 7.8, 150 mM NaCl). Proteins were saturated with excess zinc (II) chloride, allowed for samples to sit at room temperature for 15 minutes prior to running the scan. The samples were loaded in a 1 cm quartz cell containing a magnetic stirrer. The start and final temperature were 4°C and 90°C, respectively, and the scan rate was 40°C/hour. The thermo unfolding of M3M4 protein was monitored at 222 nm with temperature increments of 0.5 °C. All samples were run with reverse temperature to check for protein reversibility. All samples were run in triplicate.

The data from CD signal were reported in millidegree and was converted to θ (mdeg cm^2/dmole) by using the following equation:

$$\theta = \frac{CD\ signal\ in\ millidegree * 100}{number\ of\ residues * cuvette\ pathlength\ in\ cm * protein\ concentration}$$

2.15 Test expression of M3M4 in minimal media

To make 500 ml of minimal media, the following chemicals were added to dH_2O: 6.5g KH_2PO_4, 5 g K_2HPO_4, 4.5 g Na_2HPO_4 (anhydrous), 1.2 g K_2SO_4, 0.6 g $^{15}NH_4Cl$ (for test expression, use NH_4Cl). This medium was sterilized by autoclaving. The following nutrients were added to the 500 mL M9 minimal medium: 10 ml of 20 % (w/v) glucose, 2.5 ml of 5 mg/mL Thiamine, 1 mL of 1 M $MgSO_4$, 250 µl of 0.1 M $CaCl_2$, and 2.5 ml trace metals (50 µM $FeCl_2$, 20 µM $CaCl_2$, 10 µM each of $MnCl_2$, $ZnSO_4$, and 2 µM each of $CoCl_2$, $CuCl_2$, $NiCl_2$).

To grow *E. coli* in minimal media, the pRM3 vector was transformed into *E. coli* strain BL21 (star) DE3 pLysS 1240 (Invitrogen) and plated in LB/Agar plates with 100 ng/µl ampicillin, 34 ng/µl chloramphenicol, and 50 ng/µl spectinomycin. Colonies were picked and inoculated in 5 mL of start-up LB media cultures containing all three antibiotics. The start-up cultures were grew overnight at 37°C in a shaker. The start-up culture (1 mL) was used to inoculate a 100 mL minimal media containing all three antibiotics. The bacteria minimal media cultures were allowed to grow to log phase (0.6-0.8 OD) and induced with 0.1 or 0.2 mM IPTG overnight. The cultures were grown at 37°C on a shaker. Samples were harvest, lysed, and analyzed via western blotting. All protocols for western blotting are the same as describe above for strep-tag.

3 Results

The focus of our study is study the structure and function of specific domains in ZIP4 that are known to play a role in regulating ZIP4. The intracellular loop between transmembrane 3 and transmembrane 4 (M3M4) of ZIP4 has previously been shown to be the target site of ubiquitination in the presence of high intracellular zinc[8]. The ubiquitination of this domain leads to the degradation of the entire transporter via the lysosomal and proteosomal pathway[8]. Our goals were to see if Zn^{2+} binds to this domain and to understand the structural changes of M3M4 in the presence and absence of zinc. We hypothesized that in the presence of high intracellular zinc, free zinc cations will bind to M3M4 and induce a conformational change. A lysine residue found in this domain (K463) is highly conserved among the ZIP family[47]. Therefore we hypothesize that this residue, lysine463, is the site of ubiquitination and when zinc binds to M3M4, the conformational change exposed the lysine residue and hence ubiquitination occurs.

3.1 Expression of NS, WS, and M3M4 using pTYB2 vector

The DNA sequence of the three targeted domains (N-terminus with signal peptide (WS), N-terminus without signal peptide (NS), intracellular loop between transmembrane 3 and 4 (M3M4)) of ZIP4 were successfully cloned and inserted into the pTYB2 vector (data not shown). The vector has a chitin binding domain fused at the C-terminus along with a long intein region. The vector is under the control of the T7 promoter and has a built-in ampicillin resistance gene. The vectors were expressed using the *E. coli* strain BL21 (star) DE3 pLysS 1240 (Invitrogen). Our results showed that all three proteins (WS, NS, and M3M4) were unable to be expressed using this vector. The chitin binding protein antibody (Anti-CBD) (NEB) was nonspecific. The antibody binds to nonspecific proteins that do not match up with our target protein. We eventually determined that even in *E. coli* cells that do not carry the plasmid; anti-CBD binds to nonspecific protein. We switched to the monoclonal anti-CBD (NEB) but that showed no detections of proteins.

3.2 Expression of NS with Strep-tag

The N-terminal domain without signal peptide (NS) was cloned into the pPR-IBA1 plasmid. This vector was designated as pRNS. The vector was transformed into the *E. coli* strain BL21 (star) DE3 pLysS 1240 (Invitrogen) for protein expression. The NS protein was expressed in different conditions to optimize the expression level. Our results showed that NS was successfully expressed in our *E. coli* strain (Figure 4a) but most of the NS protein was found in inclusion bodies. In order to improve soluble protein expression, we changed the concentration of IPTG and the induction temperature; we also tried using autoinduction media and growing the *E. coli* strain in trace amount of Zn^{2+} to help facilitate proper folding of the protein. We found that the best conditions was at 37°C, 0.1 mM IPTG, in the presence of 50 µM $ZnCl_2$ gave the best protein expression of 50 % soluble protein and 50% in inclusion bodies. Affinity chromatography using strep-tactin resins was unsuccessful. The NS fused with strep-tag (II) did not bind to the resin and as a result the protein was eluted in the flow through fractions.

3.3 Expression of M3M4

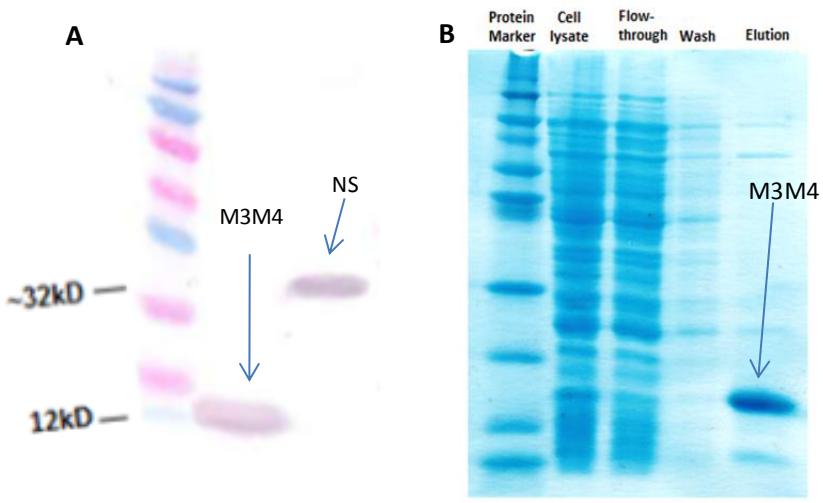

Figure 4: Protein expression
*M3M4 was expressed in BL21 E. coli cells and detected by Strep-tactinAb (IBA).M3M4 was purified by affinity chromatography (Strep-tactin resins). (**A**) Western result of protein expression, M3M4 is detected at around 12kDa. (**B**) Purification schematic of M3M4.*

Primers were designed to target specifically the in frame sequence that encodes the intracellular loop between transmembrane 3 and transmembrane 4. This domain is composed of 75 amino acids (residues 423-499) which includes a significant histidine-rich region (Figure 2). The PCR portion of the ZIP4 M3M4 gene was successfully inserted into pPR-IBA1 vector (IBA) and was expressed in BL21 *E. coli* cells. This vector encodes a 101-residue protein of which the N-terminal includes 15 residues containing the start codon methionine and residues from the vector upstream of the cut site (See Appendix A). The C-terminus of the protein contain the linker amino acids and the strep-tag. M3M4 was grown and expressed using autoinduction media overnight at 37°C[50]. This induction method produced the highest amount of M3M4 in comparison to induction with any IPTG concentration. M3M4 protein was soluble and did not agreggate. Sample lysates were loaded on SDS-PAGE and electrotransferred to a PVDF membrane. The M3M4 protein was detected using a Strep-tactin antibody (IBA). A band around 12 kDa was detected on the western blot and this corresponds to the molecular weight of M3M4 (11.1 kDa) (Figure 4A).

To further verify the expression of M3M4, preparations of protein were sent out to Iowa State Protein Facility for protein N-terminal sequencing. The results from protein N-terminal sequencing showed that the first five residues on the N-terminus of M3M4 (GDRGP) matched the first five residues of the target protein.

Gravity flow, affinity chromatography was performed to purify the expressed M3M4 protein. The column was packed with 2 mL of strep-tactin resins (IBA) and cell lysates were passed through the column. Here, we found that the optimal amount of resin is 2 mL resins for every 2.5 mg of protein. In general, 2 liters of BL21 *E. coli* culture will produce anywhere between 2 – 3 mg M3M4 protein. The M3M4 protein, which has a strep-tag at the C-terminus, binds to the resin and the column was washed with buffer W. The M3M4 protein was eluted by buffer containing 2.5 mM desthiobiotin which competitively binds to the resin. Figure 4B shows the schematic of M3M4 purification. M3M4 was further purified by the same method if not pure after the first round. The addition of two column volumes of 0.2 M ammonium sulfate after the washing step can help decrease nonspecific binding.

3.4 Zinc binding to M3M4

ZIP4 transports zinc into the cells[5, 17, 46]. When the cells have excessive zinc, it is important to stop the influx of zinc. ZIP4 is degraded when zinc level is high[8]. We hypothesize that the intracellular loop M3M4 acts as a zinc sensor so that when zinc level is high, the M3M4 loop will bind zinc and this action will signal for ubiquitination and subsequent protein degradation.

A

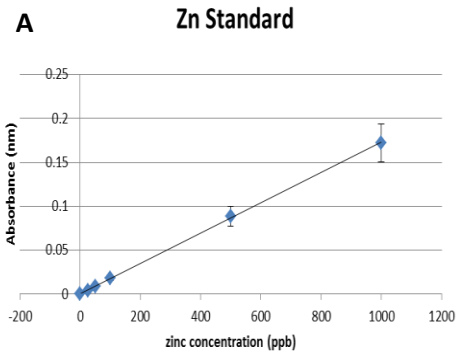

B

Average zinc concentration per 1 µM M3M4	119.3 ± 14.56 ppb
Zn:M3M4 stoichiometry	1.8 ± 0.223

Figure 5: Zn:Protein stoichiometry
The binding stoichiometry of Zn^{2+} to protein was determined by atomic absorbance. ***(A)*** *Standard zinc absorbance curve.* ***(B)*** *Zn: M3M4 stoichiometry was determined to be 1.8 ± 0.2.*

In order to understand the Zn^{2+} binding characteristics, we determined the Zn^{2+} to M3M4 binding stoichiometry. Atomic absorbance spectrophotometry (AAS) is a powerful tool used to determine metal concentration[52, 53]. Here, we apply this technique to determine the zinc concentration bound to protein. A known concentration of purified M3M4 protein was incubated with 5x excess Zn^{2+} for 15 minutes and the excess zinc was removed using the Amicon centrifugal filter device (Millipore) or passing the entire sample through a Sephadex G-25 column. The samples were treated with 1 mL of HNO_3 and heated to 95°C then subjected to a Flame-AAnalyst 700 (Perkin-Elmer) and monitored at 213.9 nm. The standard curves were constructed using a zinc standard solution prepared from stock $ZnCl_2$. Our result from AAS indicates that the average Zn^{2+} concentration per 1 µM M3M4 protein is 119.3 ± 14.56 ppb corresponding to a 1.8 ± 0.2 Zn^{2+}: 1 M3M4 stoichiometry (Figure 5A, B). This indicates that there are two zinc binding sites on M3M4.

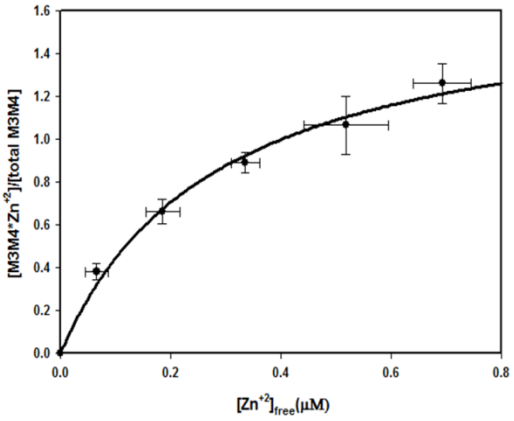

$$f = \frac{nx}{K_d(1 + \frac{x}{K_d})}$$

# of binding site (n)	1.7 ± 0.1
K_d	280 ± 50 nM
R^2	0.9921
Standard error of est.	0.0463

Figure 6: Binding affinity of Zn^{2+} to M3M4
The binding affinity of Zn^{2+} to M3M4 was determined by titration M3M4 with Zn^{2+} in the presence of Fluozin-1. The data were fitted with the equation on the right and plot was allowed to flow for best fit curve. Values are the means of 3 ± STD.

To further investigate the Zn^{2+}/M3M4 complex, the binding affinity of M3M4 for Zn^{2+} was determined by titrating the purified M3M4 protein with Zn^{2+} in the presence of Fluozin-1 (Molecular Probe; Invitrogen). Fluozin-1 forms a 1:1 indicator/zinc complex with a known K_d and the concentration of unbound zinc can be monitored by fluorescence spectrophotometry. This allows the calculation of free Zn^{2+} and Zn^{2+}-protein complex. The Zn^{2+}-protein complex was plotted against the free Zn^{2+} concentration and fitted to equation in Figure 6 using SigmaPlot. Here, we defined *f* as the molar ratio of

zinc bound to M3M4, K_d is the binding affinity of zinc to M3M4, *n* as the number of binding sites, and *x* as level of free zinc. The equation was set to fit for best fit curve and the resulting values for number of binding site is 1.7 ± 0.1 which is consistent with our zinc binding stoichiometry. From our fluorescence experiments the binding affinity of Zn^{2+} to M3M4 was determined to be 280 ± 50 nm. The nature of the fitted graph, because it is exponential and not sigmoidal, indicates that the two binding sites M3M4 are independent of each other[54].

3.5 Changes in M3M4 conformational state

Native gel electrophoresis separates protein according to both the protein mass and charge. By eliminating the denaturing factors, the protein can retain its folded conformation. Here, we applied this technique to study the conformational changes of M3M4 in the presence and absence of Zn^{2+}. M3M4 in its native conformation appears to exist in multiple conformational species. The gel shows that M3M4 in the absence of Zn^{2+} appears as two separate bands with similar molecular weight (Figure 7, lane 2). When M3M4 was saturated with Zn^{2+}, the band shifted upward. There was only one distinct band that appeared when Zn^{2+} was bound to M3M4 (Figure 7, lane 3). In the presence of Zn^{2+}, Zn^{2+} bound to M3M4 induced a conformational change. M3M4 exists only in one conformation state in the presence of Zn^{2+}.

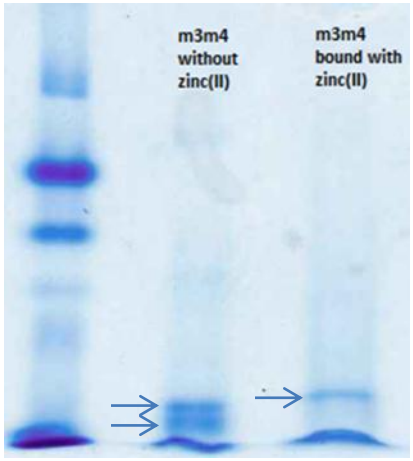

Figure 7: Native conformational state
Native gel electrophoresis was performed on M3M4. Lane 1 is the native gel marker, lane 2 is M3M4 in the absence of zinc, lane 3 is M3M4 saturated with zinc.

3.6 M3M4 secondary structure in the absence and presence of zinc

We have shown that two zinc ions bind to the M3M4 domain. The conformation state of M3M4 also changes in the presence of Zn^{2+}. In order to have a better understanding of M3M4 conformational state in the presence and absence of zinc, we examined the secondary structure of M3M4 using circular dichroism. Circular dichroism (CD) is an effective tool that applies circular polarized light to determine the secondary structure of protein[55, 56]. When a protein is folded they often have highly asymmetric secondary structural elements like α-helices and β-sheets which can be quantitated by CD. The α-helix gives off the most characteristic spectrum which have two negative bands near 222 and 208 nm whereas β-sheets have a negative band at 217 and 180 nm[55]. The secondary structure of M3M4 was measured in the absence of Zn^{2+} or saturated with Zn^{2+} by far-UV CD. M3M4 became more α-helical in the presence of Zn^{2+} as evident in the increase of negativity near 222 and 208 nm (Figure 8A) with respect to M3M4 spectra alone. In addition, the data were analyzed by K2d algorithm and it suggests that there wass a 20% increase in α-helices and 23% decrease in β-sheets when Zn^{2+} was bound to M3M4 (Figure 8B).

A

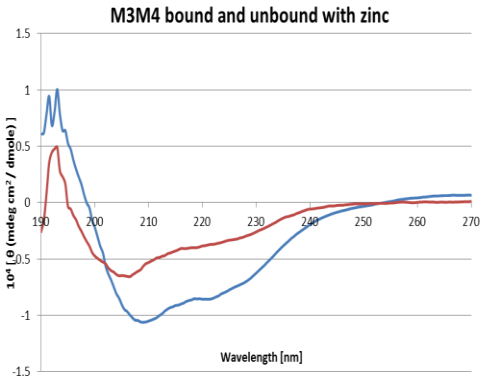

B

	M3M4 unbound	M3M4 bound to zinc
Alpha Helices	0.09	0.29
Beta Sheets	0.36	0.13
Random coils	0.55	0.59

Figure 8: Secondary structure by CD
*The secondary structure of M3M4 was scanned in the presence or absence of Zn^{2+}. (**A**) The difference in M3M4 secondary structure in the presence (blue) or absence (red) of Zn^{2+}. The spectra were normalized to the concentration of protein. (**B**) Percentage of helices, sheets, and random coils depicted by K2d algorithmic. Values are the means of 3 scans of 3 protein prep.*

3.7 Thermo unfolding of M3M4

The thermo unfolding of M3M4 was monitored by far UV CD spectroscopy at 222 nm which is proportional to the α-helical protein content. The starting temperature was 4°C and the final temperature was 90°C. Scans were taken every 0.5°C with a wait time of 80 seconds. The thermal scan obtained at 222 nm of M3M4 is shown in figure 9A and 9B in the absence and presence of zinc, respectively. The melting curve for M3M4 showed no significant transitional changes as the temperature increased. The changes of M3M4 protein could not be measure at 222 nm. This is consistent with the CD scans which showed that the M3M4 is composed of only 9 percents α-helices. Therefore detecting the transition temperature of M3M4 at 222 nm was not feasible. In the presence of Zn^{2+}, the thermo unfolding of bound M3M4 had a significant transition temperature, where the M3M4 protein unfolds (T_m) at ~57°C. Unfortunately, at the end of the run, M3M4 in the presence or absence of Zn^{2+} aggregated and precipitated out of solution. Therefore thermo refolding of M3M4 was not possible. It was unclear whether the aggregations occurred during or after the unfolding.

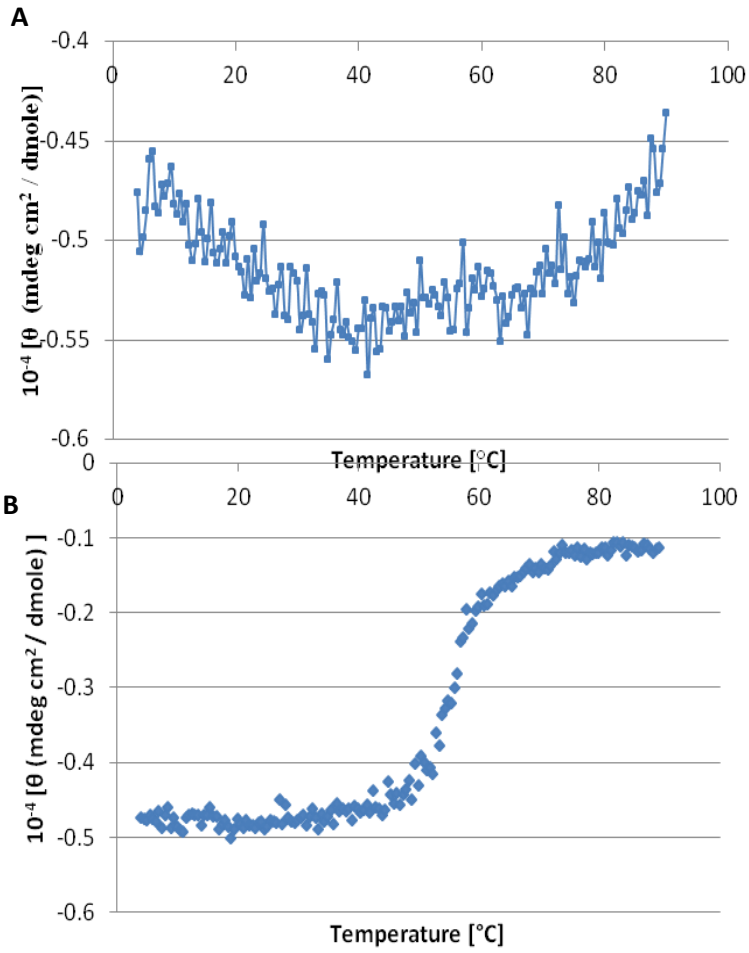

Figure 9: Thermo unfolding of M3M4
CD signal was followed at 222 nm for both scans. (**A**) Thermo unfolding of M3M4 protein in the absence of Zn. (**B**) Thermo unfolding of M3M4 protein in the presence of Zn^{2+}.

3.8 Expression of M3M4 in minimal media

Our target was to label M3M4 with ^{15}N and ^{13}C for future NMR experiments. In order to radioactively label the M3M4 protein, M3M4 was expressed in minimal media. Minimal media contain the minimum amount of nutrients necessary to grow *E. coli*[57]. Here, we were testing for the expressions of M3M4 in unlabeled minimal media with different induction conditions. *E. coli* was grow in minimal media to log phase (OD 0.6-0.8) and induced overnight with either 0.1 or 0.2 mM IPTG. Our result showed that M3M4 was successfully expressed in minimal media. There was more M3M4 expressed in the induced cultures than the negative control (no IPTG) and there was no difference in the level of protein expression between 0.1 and 0.2 mM IPTG (Figure 10).

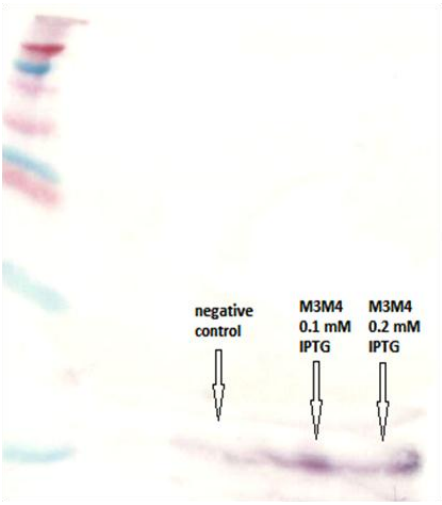

Figure 10: M3M4 expression in minimal media. *M3M4 was expressed minimal media. The cells were induced with no ITPG (- control), 0.1 mM IPTG, or 0.2 mM IPTG. Cultures were induced overnight.*

4 Discussion

ZIP4 mediates zinc uptake in enterocytes and plays an important role in zinc homeostasis[1, 5, 20]. Mutations that caused ZIP4 to malfunction result in zinc deficiency phenotypes such as AE and ZIP4 has been shown to be overexpressed in patients with pancreatic cancer[7, 30, 48]. In normally functioning cells, the surface expression of ZIP4 is inversely proportional to the level of intracellular zinc. When cells are in a zinc depleted condition, ZIP4 is recruited to the plasma membrane. In contrast, when cells are in a zinc repleted condition, ZIP4 undergoes endocytosis and circulate in the cytoplasm[5, 6, 13]. Furthermore, when there is a high level of intracellular zinc, a residue within the intracellular loop between transmembrane 3 and transmembrane 4 undergoes ubiquitination resulting in the degradation of the entire ZIP4 transporter[8]. This indicates that ZIP4 play a key role in zinc homeostasis by sensing dietary zinc level.

Most of the previous work on ZIP4 has focused on studying the ZIP4 mRNA and protein expression level *in vivo*. Here, we are interested in investigating the biophysical and biochemical processes of the intracellular loop between transmembrane 3 and 4 (M3M4). We hypothesized that this domain regulates the surface expression of ZIP4 by acting as a sensor for intracellular Zn^{2+}. Our results indicate that M3M4 binds to zinc with nanomolar affinity with a 2:1 zinc to M3M4 stoichiometry. Furthermore there is a large conformational change when zinc is bound. Our results indicates that the binding of Zn^{2+} to M3M4 is a potential mechanism in which the M3M4 domain acts as a zinc sensor and signal for ubiquitination. This is the first time in which this M3M4 region of ZIP4 is shown to bind zinc and to initiate a conformational change.

4.1 Zinc binding capability of M3M4

The M3M4 loop contains a histidine-rich region in the sequence of $^{436\text{-}}$CGHSSHSHGGHSH$^{\text{-}448}$ which is highly similar to the sequence HEXXHXXGXXH or HX_nH and has been shown to bind zinc in other zinc binding proteins such as metalloproteases and hydrolases[8, 47]. Recent data have shown that the deletion of this histidine-rich motif abolished ubiquitination[8]. Hence we hypothesize that this histidine-rich motif is the binding site for zinc. Furthermore, individual site-directed mutagenesis of each histidine does not impact ubiquitination but mutations that convert all of the histidines to alanines eliminate ubiquitination[8]. Our AAS data shows that zinc bind to M3M4 with a stoichiometry of two zinc cations for every M3M4. This could explain the reason why point mutation of a single histidine within this consensus sequence does not impact ubiquitination. The mutation of individual histidines might impact the affinity of one zinc binding site but if the second site is still functional, M3M4 still can be ubiquitinated.

We are still unclear as to why the second Zn^{2+} ion binds to M3M4. One possible explanation is that the first binding site binds zinc to indicate that there is a sufficient amount of intracellular zinc and

the binding of the second zinc ion indicates that there are more than enough intracellular zinc and that ZIP4 is no longer required. But in order for this to be true, there must be two different binding affinities. The binding affinity for the first site needs be higher so that it can detect normal intracellular zinc which is in the upper picomolar to lower nanomolar[58]. The second site should have a lower binding affinity to detect the rise in intracellular zinc (high nanomolar to micromolar). Our result indicates that the two binding sites are independent of each other. The experiments were measured in the micromolar zinc concentration consequently we might have already saturated the first binding site.

The affinity of the M3M4 domain of ZIP4 for zinc is an important parameter in understanding how M3M4 regulates the ZIP4 transporter. A major goal of this project was to determine the affinity of M3M4 for Zn^{2+}. This was achieved by titrating zinc in the presence of a metallochromic indicator. Using fluorescence spectroscopy, we determined the binding affinity (K_d) of M3M4 to zinc is 280 ± 50 nM which corresponds to an association constant of 3.6 $x10^6 M^{-1}$. This has a low affinity compared to other protein/zinc binding complexes, which have affinities in the picomolar range[58]. This can be explained by M3M4 acting as a sensor to detect an increase in cytosolic Zn^{2+} level. The binding affinity of M3M4 for Zn^{2+} is in the upper limit of free Zn^{2+} so that it does not compete with other intracellular proteins which require Zn^{2+} for proper function.

We acknowledge that this is an *in vitro* experiment and that only the 75 residues of the entire protein are expressed hence there are multiple factors that could lead to a deviation in the affinity when compared to the full length protein. First, the expression of only M3M4 means that there are no N- and C-terminus constraints of the transmembrane in the full length protein so the binding affinity will be different. There could also be other proteins such as chaperones that facilitate the binding of Zn^{2+} to M3M4. But here, we are only interested in whether or not this specific region binds to Zn^{2+} and what happens to the structure of this protein when it binds Zn^{2+}. Considering that the upper limit of cytosolic

zinc is nanomolar, our K_d (280 ± 50 nm) of the M3M4 domain appears to be a physiological relevant value.

4.2 The conformational change of M3M4

ZIP4 is regulated in response to intracellular zinc level[5, 8, 43, 59]. An analysis of the changes in ZIP4 M3M4 protein structure can help in understanding how ZIP4 response to the level of zinc. Here, by circular dichroism we showed that M3M4 binds to Zn^{2+} resulting in a conformational change. We showed that in the presence of Zn^{2+}, M3M4 become more helical. In fact, K2d analysis depicted a 20 percent increase in helical content compared to M3M4 without Zn^{2+}. It has been shown previously in proteins with zinc finger domain, such as transcription factor IIIA, that upon addition of Zn^{2+} zinc finger domain changed from a less well-defined structure to a more well-defined structure[60].

There is a lysine residue (K463) on the M3M4 domain that is conserved in throughout the ZIP family[8, 47]. Therefore we hypothesize that this residue could be the site for ubiquitination. When Zn^{2+} binds to the M3M4 domain, the conformational change exposes this lysine residue which signals for ubiquitination.

4.3 Future implications

This is the first study to show that the M3M4 domain binds zinc and that the binding of zinc leads to a conformational change. This is a significant insight into the role in which Zn^{2+} plays in regulating the surface expression of ZIP transporters. One common feature among the ZIP family is the long intracellular loop between transmembrane 3 and 4. The length and residues in this domain are not well conserved but most have the histidine-rich motif with the sequence $(HX)_n$ where n= 3-6 and a conserved lysine residue[47]. Therefore, we propose that this intracellular loop of ZIP family acts as a zinc

sensor where the difference in length and the different residues in the histidine-rich motif could give rise to difference in affinity among this family of protein.

In the presence of high intracellular zinc concentration, this loop binds to zinc to induce a conformational change exposing the lysine residue for ubiquitination. By degrading ZIP4, the cells can regulate the amount of additional zinc entering the cells. This could be a mechanism in which the cells take to protect itself from zinc toxicity. In pancreatic cancer cells, the upregulation of ZIP4 leads to increase in cell proliferation and tumor progression[7, 48]. The detail mechanisms of how ZIP4 regulates cancer cell growth are still unclear. Recent data showed that the overexpression of ZIP4 caused CREB to be phosphorylated and increased the transcription and secretion of IL-6 which activates STAT3 to lead to cyclin D1 expression increase resulting in the increase of cancer cell growth[61].

Further studies are needed to be performed on this domain in order to have a better understanding of the role of this domain. It would be nice to whether M3M4 coordinates other metals. There are studies that shown that ZIP4 is responsive to high level of cadmium (II)[8]. In the presence of high cadmium concentrations, ZIP4 is also degraded[8]. Though, the degradation of ZIP4 requires a much higher concentration of cadmium than zinc[8]. By comparing the binding affinity of zinc to other metals, we can have a better understanding of the specificity and selectivity of ZIP4 to zinc and other metals. It would also be interesting to look at the binding affinity of M3M4 to Zn^{2+} at different pH. It has been shown that histidine binds to Zn^{2+} more efficiently at a higher pH since the side chain of histidine is deprotonated more rapidly[62].

Appendix A – pRM3 plasmid map

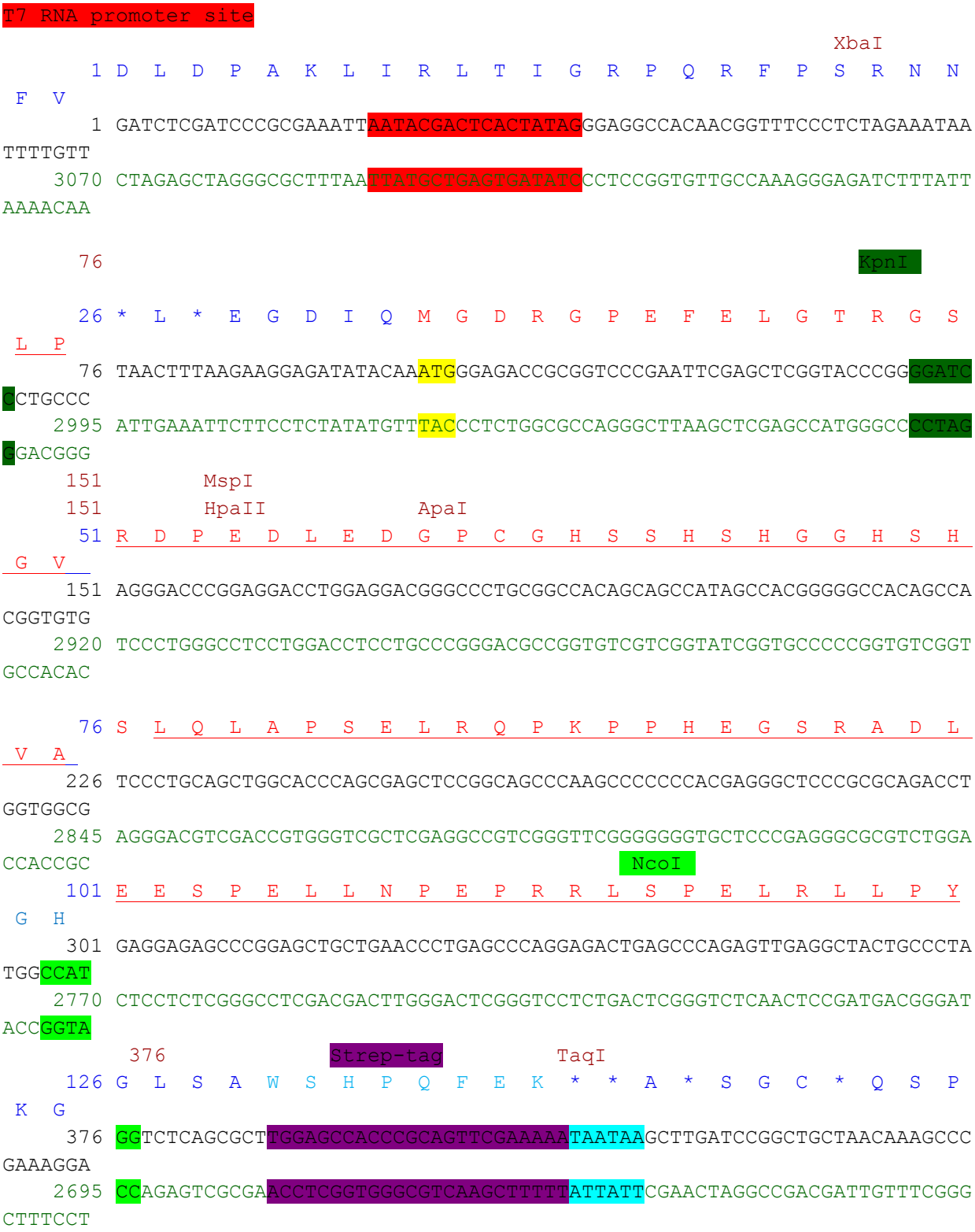

References

(1) John, E.; Laskow, T. C.; Buchser, W. J.; Pitt, B. R.; Basse, P. H.; Butterfield, L. H.; Kalinski, P.; Lotze, M. T. Zinc in innate and adaptive tumor immunity. *J. Transl. Med.* **2010***, 8*, 118.

(2) Vallee, B. L.; Auld, D. S. Zinc coordination, function, and structure of zinc enzymes and other proteins. *Biochemistry* **1990***, 29*, 5647-5659.

(3) Truong-Tran, A. Q.; Ho, L. H.; Chai, F.; Zalewski, P. D. Cellular zinc fluxes and the regulation of apoptosis/gene-directed cell death. *J. Nutr.* **2000***, 130*, 1459S-66S.

(4) Rink, L.; Kirchner, H. Zinc-altered immune function and cytokine production. *J. Nutr.* **2000***, 130*, 1407S-11S.

(5) Andrews, G. K. Regulation and function of Zip4, the acrodermatitis enteropathica gene. *Biochem. Soc. Trans.* **2008***, 36*, 1242-1246.

(6) Kambe, T.; Andrews, G. K. Novel proteolytic processing of the ectodomain of the zinc transporter ZIP4 (SLC39A4) during zinc deficiency is inhibited by acrodermatitis enteropathica mutations. *Mol. Cell. Biol.* **2009***, 29*, 129-139.

(7) Li, M.; Zhang, Y.; Liu, Z.; Bharadwaj, U.; Wang, H.; Wang, X.; Zhang, S.; Liuzzi, J. P.; Chang, S. M.; Cousins, R. J.; Fisher, W. E.; Brunicardi, F. C.; Logsdon, C. D.; Chen, C.; Yao, Q. Aberrant expression of zinc transporter ZIP4 (SLC39A4) significantly contributes to human pancreatic cancer pathogenesis and progression. *Proc. Natl. Acad. Sci. U. S. A.* **2007***, 104*, 18636-18641.

(8) Mao, X.; Kim, B. E.; Wang, F.; Eide, D. J.; Petris, M. J. A histidine-rich cluster mediates the ubiquitination and degradation of the human zinc transporter, hZIP4, and protects against zinc cytotoxicity. *J. Biol. Chem.* **2007***, 282*, 6992-7000.

(9) Pickart, C. M.; Eddins, M. J. Ubiquitin: structures, functions, mechanisms. *Biochim. Biophys. Acta* **2004***, 1695*, 55-72.

(10) Creighton, T. E. In *Relationship between Protein Conformation and Binding;* Proteins; W.H. Freeman and Company: New York, 1993; pp 348.

(11) Ackland, M. L.; Michalczyk, A. Zinc Deficiency and Its Inherited Disorders - A Review. *Genes Nutr.* **2006**, 1, 41-9.

(12) Moynahan, E. J.; Johnson, F. R.; McMinn, R. M. H. Acrodermatitis Enteropathica: Demonstration of Possible Intestinal Enzyme Defect. *Proc. R. Soc. Med.* **1962***, 55*, 300.

(13) Wang, K.; Zhou, B.; Kuo, Y. M.; Zemansky, J.; Gitschier, J. A novel member of a zinc transporter family is defective in acrodermatitis enteropathica. *Am. J. Hum. Genet.* **2002***, 71*, 66-73.

(14) Schmitt, S.; Kury, S.; Giraud, M.; Dreno, B.; Kharfi, M.; Bezieau, S. An update on mutations of the SLC39A4 gene in acrodermatitis enteropathica. *Hum. Mutat.* **2009***, 30*, 926-933.

(15) Wang, K.; Pugh, E. W.; Griffen, S.; Doheny, K. F.; Mostafa, W. Z.; al-Aboosi, M. M.; el-Shanti, H.; Gitschier, J. Homozygosity mapping places the acrodermatitis enteropathica gene on chromosomal region 8q24.3. *Am. J. Hum. Genet.* **2001***, 68*, 1055-1060.

(16) Liuzzi, J. P.; Cousins, R. J. Mammalian zinc transporters. *Annu. Rev. Nutr.* **2004***, 24*, 151-172.

(17) Sekler, I.; Sensi, S. L.; Hershfinkel, M.; Silverman, W. F. Mechanism and regulation of cellular zinc transport. *Mol. Med.* **2007***, 13*, 337-343.

(18) Sensi, S. L.; Paoletti, P.; Bush, A. I.; Sekler, I. Zinc in the physiology and pathology of the CNS. *Nat. Rev. Neurosci.* **2009***, 10*, 780-791.

(19) Cousins, R. J.; Liuzzi, J. P.; Lichten, L. A. Mammalian zinc transport, trafficking, and signals. *J. Biol. Chem.* **2006***, 281*, 24085-24089.

(20) King, J. C.; Shames D.M.; Woodhouse L.R. Zinc Homeostasis in Humans. *JN* **2000***, 130*, 1360.

(21) Coyle, P.; Philcox, J. C.; Carey, L. C.; Rofe, A. M. Metallothionein: the multipurpose protein. *Cell Mol. Life Sci.* **2002***, 59*, 627-647.

(22) Lu, M.; Chai, J.; Fu, D. Structural basis for autoregulation of the zinc transporter YiiP. *Nat. Struct. Mol. Biol.* **2009***, 16*, 1063-1067.

(23) Lichten, L. A.; Cousins, R. J. Mammalian zinc transporters: nutritional and physiologic regulation. *Annu. Rev. Nutr.* **2009***, 29*, 153-176.

(24) Mocchegiani, E.; Malavolta, M.; Costarelli, L.; Giacconi, R.; Cipriano, C.; Piacenza, F.; Tesei, S.; Basso, A.; Pierpaoli, S.; Lattanzio, F. Zinc, metallothioneins and immunosenescence. *Proc. Nutr. Soc.* **2010***, 69*, 290-299.

(25) Liuzzi, J. P.; Bobo, J. A.; Lichten, L. A.; Samuelson, D. A.; Cousins, R. J. Responsive transporter genes within the murine intestinal-pancreatic axis form a basis of zinc homeostasis. *Proc. Natl. Acad. Sci. U. S. A.* **2004***, 101*, 14355-14360.

(26) Palmiter, R. D.; Findley, S. D. Cloning and functional characterization of a mammalian zinc transporter that confers resistance to zinc. *EMBO J.* **1995***, 14*, 639-649.

(27) Palmiter, R. D. Protection against zinc toxicity by metallothionein and zinc transporter 1. *Proc. Natl. Acad. Sci. U. S. A.* **2004***, 101*, 4918-4923.

(28) Kim, B. E.; Wang, F.; Dufner-Beattie, J.; Andrews, G. K.; Eide, D. J.; Petris, M. J. Zn2+-stimulated endocytosis of the mZIP4 zinc transporter regulates its location at the plasma membrane. *J. Biol. Chem.* **2004***, 279*, 4523-4530.

(29) Kelleher, S. L.; Lopez, V.; Lonnerdal, B.; Dufner-Beattie, J.; Andrews, G. K. Zip3 (Slc39a3) functions in zinc reuptake from the alveolar lumen in lactating mammary gland. *Am. J. Physiol. Regul. Integr. Comp. Physiol.* **2009***, 297*, R194-201.

(30) Maverakis, E.; Fung, M. A.; Lynch, P. J.; Draznin, M.; Michael, D. J.; Ruben, B.; Fazel, N. Acrodermatitis enteropathica and an overview of zinc metabolism. *J. Am. Acad. Dermatol.* **2007***, 56*, 116-124.

(31) Palmiter, R. D.; Cole, T. B.; Findley, S. D. ZnT-2, a mammalian protein that confers resistance to zinc by facilitating vesicular sequestration. *EMBO J.* **1996***, 15*, 1784-1791.

(32) Palmiter, R. D.; Cole, T. B.; Quaife, C. J.; Findley, S. D. ZnT-3, a putative transporter of zinc into synaptic vesicles. *Proc. Natl. Acad. Sci. U. S. A.* **1996***, 93*, 14934-14939.

(33) Huang, L.; Gitschier, J. A novel gene involved in zinc transport is deficient in the lethal milk mouse. *Nat. Genet.* **1997***, 17*, 292-297.

(34) Kambe, T.; Narita, H.; Yamaguchi-Iwai, Y.; Hirose, J.; Amano, T.; Sugiura, N.; Sasaki, R.; Mori, K.; Iwanaga, T.; Nagao, M. Cloning and characterization of a novel mammalian zinc transporter, zinc transporter 5, abundantly expressed in pancreatic beta cells. *J. Biol. Chem.* **2002***, 277*, 19049-19055.

(35) Lyubartseva, G.; Smith, J. L.; Markesbery, W. R.; Lovell, M. A. Alterations of zinc transporter proteins ZnT-1, ZnT-4 and ZnT-6 in preclinical Alzheimer's disease brain. *Brain Pathol.* **2010***, 20*, 343-350.

(36) Kirschke, C. P.; Huang, L. ZnT7, a novel mammalian zinc transporter, accumulates zinc in the Golgi apparatus. *J. Biol. Chem.* **2003***, 278*, 4096-4102.

(37) Chimienti, F.; Devergnas, S.; Favier, A.; Seve, M. Identification and cloning of a beta-cell-specific zinc transporter, ZnT-8, localized into insulin secretory granules. *Diabetes* **2004***, 53*, 2330-2337.

(38) Chimienti, F.; Devergnas, S.; Pattou, F.; Schuit, F.; Garcia-Cuenca, R.; Vandewalle, B.; Kerr-Conte, J.; Van Lommel, L.; Grunwald, D.; Favier, A.; Seve, M. In vivo expression and functional characterization of the zinc transporter ZnT8 in glucose-induced insulin secretion. *J. Cell. Sci.* **2006***, 119*, 4199-4206.

(39) Franklin, R. B.; Ma, J.; Zou, J.; Guan, Z.; Kukoyi, B. I.; Feng, P.; Costello, L. C. Human ZIP1 is a major zinc uptake transporter for the accumulation of zinc in prostate cells. *J. Inorg. Biochem.* **2003***, 96*, 435-442.

(40) Gaither, L. A.; Eide, D. J. Functional expression of the human hZIP2 zinc transporter. *J. Biol. Chem.* **2000***, 275*, 5560-5564.

(41) Kelleher, S. L.; Lopez, V.; Lonnerdal, B.; Dufner-Beattie, J.; Andrews, G. K. Zip3 (Slc39a3) functions in zinc reuptake from the alveolar lumen in lactating mammary gland. *Am. J. Physiol. Regul. Integr. Comp. Physiol.* **2009***, 297*, R194-201.

(42) Weaver, B. P.; Dufner-Beattie, J.; Kambe, T.; Andrews, G. K. Novel zinc-responsive post-transcriptional mechanisms reciprocally regulate expression of the mouse Slc39a4 and Slc39a5 zinc transporters (Zip4 and Zip5). *Biol. Chem.* **2007***, 388*, 1301-1312.

(43) Dufner-Beattie, J.; Kuo, Y. M.; Gitschier, J.; Andrews, G. K. The adaptive response to dietary zinc in mice involves the differential cellular localization and zinc regulation of the zinc transporters ZIP4 and ZIP5. *J. Biol. Chem.* **2004***, 279*, 49082-49090.

(44) Taylor, K. M.; Morgan, H. E.; Johnson, A.; Hadley, L. J.; Nicholson, R. I. Structure-function analysis of LIV-1, the breast cancer-associated protein that belongs to a new subfamily of zinc transporters. *Biochem. J.* **2003***, 375*, 51-59.

(45) Hogstrand, C.; Kille, P.; Nicholson, R. I.; Taylor, K. M. Zinc transporters and cancer: a potential role for ZIP7 as a hub for tyrosine kinase activation. *Trends Mol. Med.* **2009***, 15*, 101-111.

(46) Schmitt, S.; Kury, S.; Giraud, M.; Dreno, B.; Kharfi, M.; Bezieau, S. An update on mutations of the SLC39A4 gene in acrodermatitis enteropathica. *Hum. Mutat.* **2009***, 30*, 926-933.

(47) Taylor, K. M.; Nicholson, R. I. The LZT proteins; the LIV-1 subfamily of zinc transporters. *Biochim. Biophys. Acta* **2003***, 1611*, 16-30.

(48) Li, M.; Zhang, Y.; Bharadwaj, U.; Zhai, Q. J.; Ahern, C. H.; Fisher, W. E.; Brunicardi, F. C.; Logsdon, C. D.; Chen, C.; Yao, Q. Down-regulation of ZIP4 by RNA interference inhibits pancreatic cancer growth and increases the survival of nude mice with pancreatic cancer xenografts. *Clin. Cancer Res.* **2009***, 15*, 5993-6001.

(49) Dufner-Beattie, J.; Weaver, B. P.; Geiser, J.; Bilgen, M.; Larson, M.; Xu, W.; Andrews, G. K. The mouse acrodermatitis enteropathica gene Slc39a4 (Zip4) is essential for early development and heterozygosity causes hypersensitivity to zinc deficiency. *Hum. Mol. Genet.* **2007***, 16*, 1391-1399.

(50) Studier, F. W. Protein production by auto-induction in high density shaking cultures. *Protein Expr. Purif.* **2005***, 41*, 207-234.

(51) Bradford, M. M. A rapid and sensitive method for the quantitation of microgram quantities of protein utilizing the principle of protein-dye binding. *Anal. Biochem.* **1976***, 72*, 248-254.

(52) Liska, S. K.; Kerkay, J.; Pearson, K. H. Determination of zinc and copper in urine using Zeeman effect flame atomic absorption spectroscopy. *Clin. Chim. Acta* **1985***, 151*, 231-236.

(53) Chekri, R.; Noel, L.; Vastel, C.; Millour, S.; Kadar, A.; Guerin, T. Determination of calcium, magnesium, sodium, and potassium in foodstuffs by using a microsampling flame atomic absorption spectrometric method after closed-vessel microwave digestion: method validation. *J. AOAC Int.* **2010***, 93*, 1888-1896.

(54) Garrett, R. H.; Grisham, C. M. In *Enzyme Regulation;* **Biochemistry**; Brooks/Cole, Cengage Learning, 2001; pp 456.

(55) Woody, R. W. Circular dichroism spectrum of peptides in the poly(Pro)II conformation. *J. Am. Chem. Soc.* **2009***, 131*, 8234-8245.

(56) Woody, R. W. Circular dichroism of protein-folding intermediates. *Methods Enzymol.* **2004***, 380*, 242-285.

(57) Paliy, O.; Gunasekera, T. S. Growth of E. coli BL21 in minimal media with different gluconeogenic carbon sources and salt contents. *Appl. Microbiol. Biotechnol.* **2007***, 73*, 1169-1172.

(58) Atar, D.; Backx, P. H.; Appel, M. M.; Gao, W. D.; Marban, E. Excitation-transcription coupling mediated by zinc influx through voltage-dependent calcium channels. *J. Biol. Chem.* **1995***, 270*, 2473-2477.

(59) Huang, Z. L.; Dufner-Beattie, J.; Andrews, G. K. Expression and regulation of SLC39A family zinc transporters in the developing mouse intestine. *Dev. Biol.* **2006***, 295*, 571-579.

(60) Lippard, S. J.; Berg, J. M. In *Metal Ion Folding and Cross-Linking of Biomolecules;* Principles of Bioinorganic Chemistry; University Science Books: Mill Valley, CA, 1994; pp 175.

(61) Zhang, Y.; Bharadwaj, U.; Logsdon, C. D.; Chen, C.; Yao, Q.; Li, M. ZIP4 regulates pancreatic cancer cell growth by activating IL-6/STAT3 pathway through zinc finger transcription factor CREB. *Clin. Cancer Res.* **2010***, 16*, 1423-1430.

(62) Bertini, I.; Luchinat, C. In *The reaction pathways of zinc enzymes and related biological catalysts;* Bertini, I., Gray, H. B., Lippard, S. J. and Valentine, J. S., Eds.; Bioinorganic Chemistry; University Science Books: Mill Valley, Ca, pp 175-210.